Microfluid Nanofluid (2010) 9:1–16
DOI 10.1007/s10404-010-0602-7

REVIEW

Particle focusing in microfluidic devices

Xiangchun Xuan · Junjie Zhu · Christopher Church

Received: 16 January 2010 / Accepted: 15 March 2010 / Published online: 30 March 2010

Abstract Focusing particles (both biological and synthetic) into a tight stream is usually a necessary step prior to counting, detecting, and sorting them. The various particle focusing approaches in microfluidic devices may be conveniently classified as sheath flow focusing and sheathless focusing. Sheath flow focusers use one or more sheath fluids to pinch the particle suspension and thus focus the suspended particles. Sheathless focusers typically rely on a force to manipulate particles laterally to their equilibrium positions. This force can be either externally applied or internally induced by channel topology. Therefore, the sheathless particle focusing methods may be further classified as active or passive by the nature of the forces involved. The aim of this article is to introduce and discuss the recent developments in both sheath flow and sheathless particle focusing approaches in microfluidic devices.

Keywords Particle focusing · Microfluidics · Review · Sheath flow · Dielectrophoresis · Inertia

1 Introduction

Microfluidic devices have been increasingly used over the past decade to manipulate particles (both biological and synthetic) due to the reduced sample and reagent use, enhanced efficiency, shorter processing times, and various other advantages (Toner and Irimia 2005; Yi et al. 2006; Sims and Allbritton 2007; Tanaka et al. 2007). In many of these devices, such as microflow cytometers (Huh et al. 2005; Chung and Kim 2007; Ateya et al. 2008; Godin et al. 2008) and continuous-flow sorters (Pamme 2007; Kersaudy-Kerhoas et al. 2008; Kulrattanarak et al. 2008; Tsutsui and Ho 2009), focusing particles into a tight stream is usually a necessary step prior to counting, detecting, and sorting them. Focusing particles to the center of a channel also prevents them from being adsorbed to channel walls.

As traditionally defined, particles can be focused in either two-dimensional (2D) or three-dimensional (3D). A 2D focusing normally indicates the horizontal focusing of particles to the center plane of a microchannel, where particles still scatter over the channel depth. This focusing is usually sufficient for continuous-flow particle sorters even though the adsorption of particles to the top and bottom channel walls may sometimes become an issue (Pamme 2007; Kersaudy-Kerhoas et al. 2008; Kulrattanarak et al. 2008; Tsutsui and Ho 2009). For the application to flow cytometers, however, 2D focusing frequently suffers from some problems such as the probability of coincident events due to the translocation of two or more particles past the detection region at the same time, and the variance of the detected signals from particles passing through the sensor at different heights, etc. (Huh et al. 2005; Chung and Kim 2007; Ateya et al. 2008; Godin et al. 2008). These problems are not encountered in 3D focusing, where particles are focused in both the horizontal and the vertical directions.

The simplest approach to particle focusing is driving the particle solution through a converging microchannel whose small passage ensures particles to travel in a single file (Chau et al. 1999; Fu et al. 1999; Lee et al. 2003). This method is, however, only applicable to dilute particle solutions, and so the particle throughput is very limited. Various other particle focusing methods have been

X. Xuan (✉) · J. Zhu · C. Church
Department of Mechanical Engineering, Clemson University, Clemson, SC 29634-0921, USA
e-mail: xcxuan@clemson.edu

developed in microfluidic devices, which may be conveniently classified as sheath flow focusing and sheathless focusing. Sheath flow focusers use one or more sheath fluids to pinch the particle suspension flow and thus focuses the suspended particles. Sheathless focusers achieve particle focusing in a pressure-driven or electrokinetic suspension flow by the use of either an externally applied or an internally induced force field (Huh et al. 2005; Chung and Kim 2007; Ateya et al. 2008; Godin et al. 2008).

This article is aimed to review and discuss the recent developments in both sheath flow and sheathless particle focusing approaches in microfluidic devices. Wherever applicable, the applications of the introduced particle focusing method to, for example, particle detection in microflow cytometers and particle separation in continuous-flow sorters, will also be included. In addition, readers are suggested to read the recent review papers from Huh et al. (2005), Chung and Kim (2007), Ateya et al. (2008), Godin et al. (2008), and Mao and Huang (2008).

2 Sheath flow focusing of particles

Among the diverse particle focusing methods, sheath flow focusing may be the most common one that has been adopted in microfluidic devices. This type of focusing has been realized by using either pressure-driven (Lee et al. 2006; Chang et al. 2007; Rodriguez-Trujillo et al. 2007; Tsai et al. 2008; Kummrow et al. 2009) or electric field-driven (Fu et al. 2004; Yang et al. 2005; Xuan and Li 2005; Kohlheyer et al. 2008) particle-free sheath flows to pinch the particle suspension flow and thus focus particles into a single file. In general, one or more sheath fluids should be used in order to obtain a 2D or 3D particle focusing. The various designs of microfluidic sheath flow focusing of particles that were reported before 2008 have been reviewed recently by several research groups (Huh et al. 2005; Chung and Kim 2007; Ateya et al. 2008; Godin et al. 2008). Therefore, our attention on this category of particle focusing is primarily paid to the designs that have been presented since 2008 with emphasis on those incorporating novel focusing principles and/or novel configurations.

2.1 Sheath flow focusing using grooved microchannels

Typical designs capable of 3D hydrodynamic focusing require multiple sheath inputs and several alignment steps, which complicates the device fabrication and operation. Recently, Howell et al. (2008) proposed a 3D sheath flow focusing method by the use of grooved microchannels. They reported a stripe-based design and a chevron-based design. In the latter (see Fig. 1a for a schematic), the two equal sheath flows first place the sample stream in the center of the channel, leading to a typical 2D sheath flow focusing. Then, pairs of chevrons cut into the top and bottom walls of the channel direct sheath fluid from the sides to the middle over and under the sample stream. This isolates the sample stream from the top and bottom walls of the channel, creating a vertical focusing. The height and width of thus focused sample stream can be controlled by the number of chevron pairs and the sheath-to-sample flow-rate ratio, respectively. Figure 1b shows the numerically predicted size and shape of the sample stream at different flow-rate ratios for a design with four chevron pairs, which agree closely with the experimental observations in Fig. 1c.

The chevron-based 3D sheath flow focusing has been demonstrated to focus 5.6-μm-diameter polystyrene beads at a flow rate of 10 μl/min (Golden et al. 2009). This 3D particle focuser has also been integrated into a microflow cytometer for multiplexed detection of bacteria and toxins coated onto the bead surfaces (Kim et al. 2009; Golden et al. 2009). In another design of sheath flow focusing for microfluidic flow cytometers, a micro-weir structure is positioned right beneath optical detection system (Fu et al. 2008). This structure was demonstrated to result in the separation of 5-μm- and 10-μm-diameter polystyrene beads in the vertical direction, which ensures a sequential flow of both sizes of particles through the interrogation region for a reliable detection (Tsai et al. 2008; Hou et al. 2009). The reported flow rate of their aqueous sample is approximately 14 μl/min (Hou et al. 2009).

2.2 Dean flow-assisted sheath flow focusing

Dean flow is a secondary transverse flow (characterized by two counter-rotating vortices, i.e., so-called Dean vortices) induced by centrifugal effects in a curved channel (Berger et al. 1983). Mao et al. (2007) first exploited this flow to implement a 3D hydrodynamic focusing in a single-layer planar microfluidic device. In their device, the sample flow was first vertically focused by the Dean vortices formed in a co-infused sheath flow through a 90° curve, and then horizontally focused to the center of a straight channel by two horizontal sheath flows. The vertical focusing of the sample flow was verified through a side-view imaging. This 3D hydrodynamic particle focuser has been recently integrated by the same group with a laser-induced fluorescence detection system. The system was demonstrated to provide effective high-through flow cytometry measurements of 7.32-μm- and 8.32-μm-diameter polystyrene beads at a rate of greater than 1,700 particles/s (Mao et al. 2009).

More recently, Lee et al. (2009) reported a 3D hydrodynamic focusing in a single-layer microfluidic device with only one sheath fluid. This Dean flow-assisted sheath flow

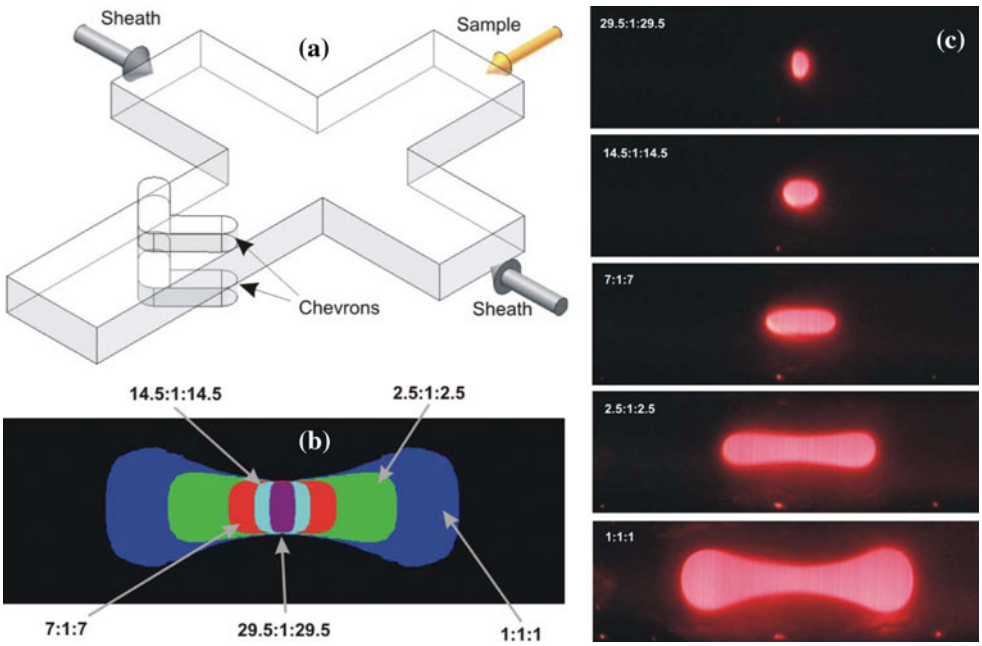

Fig. 1 **a** Isometric schematic of the chevron-based sheath flow design; **b** numerically predicted size and shape of the sample cross-section at different sheath-to-sample flow-rate ratios for a design of four pair of chevrons; **c** experimentally observed sample cross-sections. Reprinted from Howell et al. (2008) with permission from Royal Society of Chemistry

focusing took place in a microchannel comprised of an array of contraction and expansion regions. As shown schematically in Fig. 2a, the sample and sheath fluids co-flowing in the expansion region are influenced by the Dean vortices formed at the contraction region. As a consequence, the sheath fluid vertically wraps the sample fluid from both the top and bottom directions. Meanwhile, the vertically focused sample fluid drifts toward the outer corner of contraction region due to the Dean flow, resulting in a horizontal focusing. This simple device was demonstrated to implement a 3D focusing of human red blood cells in phosphate buffered saline at a flow rate of 0.1 ml/h; see Fig. 2b. The position of the focused cell stream can be easily controlled by modulating the flow rate or the number of the contraction regions.

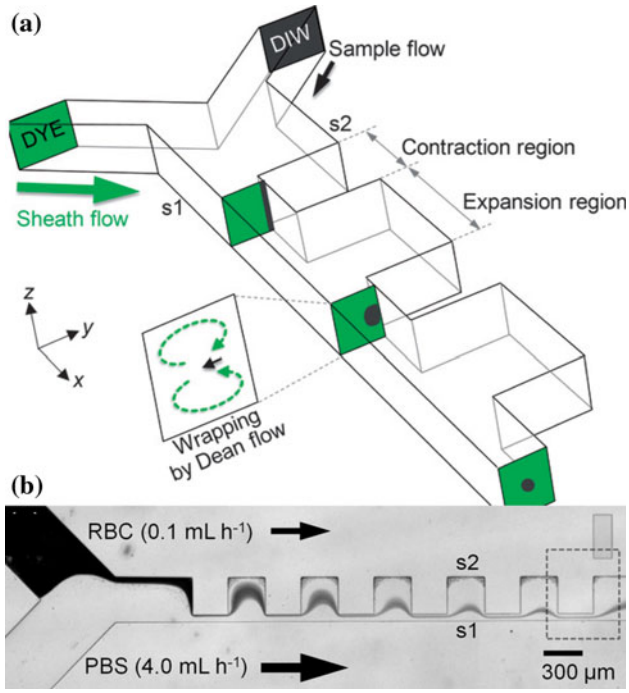

Fig. 2 **a** Schematic of the contraction–expansion array microchannel for 3D hydrodynamic focusing; **b** image of red blood cells focused by a phosphate buffered saline flow in the *xy* plane. Reprinted from Lee et al. (2009) with permission from Royal Society of Chemistry

2.3 Sheath flow focusing with vertical confinement

With sheath flow focusing, particles are typically focused to a stream traveling along the center plane (2D focusing) or centerline (3D focusing) of a microchannel for the best optical interrogation. In some applications, however, particles may be desired to flow in close proximity to, for example, the sensing electrodes deposited on the channel floor for increased signal-to-noise ratio. Such vertical confinement can be achieved using a 2D horizontal sheath flow focusing with a stepped outlet channel (Scott et al. 2008). Another means is to use a third sheath to vertically squeeze the particle stream. As shown schematically in Fig. 3, the 2D sheaths force particles in the sample stream to move in a single file manner, and the 3D sheath ensures the particles to translocate close to the sensing electrodes (Watkins et al. 2009). This device has been demonstrated to count T lymphocytes at a flow rate of 4 μl/min (with up to 8,000 cells/min) and to differentiate between live and dead/dying lymphocyte populations. In addition, a 3D hydrodynamic focusing device sharing a similar principle to Watkins et al. (2009)'s has been developed and

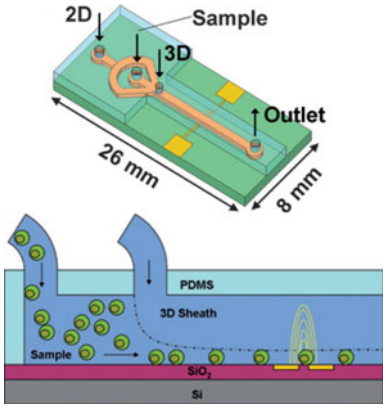

Fig. 3 (*Top*) Chip-level view of the 3D sheath flow focusing and electrical sensing region (not drawn to scale); (*bottom*) schematic of the 3D sheath flow focusing of particles with vertical confinement. Reprinted from Watkins et al. (2009) with permission from Royal Society of Chemistry

researched by Hairer and collaborators (Hairer et al. 2008; Hairer and Vellekoop 2009).

2.4 Summary of sheath flow focusing

Compared to other force-based sheathless focusing approaches whose focusing capability normally varies with the particle size, sheath flow focusing is mostly determined by the flow-rate ratio between the sheath fluid and the particle suspension and thus potentially able to focus very small particles and even molecules. Moreover, both the location and the dimension of the focused particle stream are readily tunable, which can be achieved by adjusting the flow rate of each of the sheath fluids such as the devices developed by Howell et al. (2008) and Lee et al. (2009). Accordingly, however, the requirement of sheath flow(s) complicates the device control, increases the device operation cost (due to, for example, the consumption of sheath fluids), and dilutes the particle concentration as well.

3 Sheathless focusing of particles

Sheathless particle focusers typically rely on a force to manipulate the suspended particles laterally to their equilibrium positions. This force can be either externally applied such as acoustic (Mao and Huang 2008), dielectrophoretic (Gascoyne and Vykoukal 2002), magnetic (Liu et al. 2009), and optical (Zhao et al. 2007) forces, or internally induced by channel topology including hydrophoretic (Choi et al. 2008), inertial (Di Carlo 2009), and dielectrophoretic (Zhu and Xuan 2009a) forces, etc. Therefore, the sheathless particle focusing approaches may be further classified as active or passive by the nature of the forces involved. These two sub-categories of microfluidic sheathless particle focusers are reviewed separately in the following sections.

3.1 Active sheathless focusing

3.1.1 Acoustic focusing

Acoustic focusing arises from the lateral action of acoustic wave-induced radiation pressure on particles, which forces particles toward either the pressure nodes or antinodes depending on the density and compressibility of the particle and the medium. Petersson et al. (2005) utilized the lateral acoustophoretic motion to focus both 5-μm-diameter polyamide spheres and red blood cells in a pressure-driven laminar flow. The reported flow rate of the particle suspension is 100 μl/min. The standing acoustic wave was generated by a piezoceramic plate integrated into a silicon chip. This focusing was utilized to demonstrate both a medium exchange (Petersson et al. 2005) and a continuous separation (Petersson et al. 2007) of polystyrene beads and blood cells by size and density. Goddard et al. (2006, 2007) used the ultrasonic acoustic energy to focus particles to the center of a flow stream for analysis by flow cytometry. The ultrasonic field was generated by a piezoceramic crystal attached to the external surface of a glass capillary tube. Both 7.8 μm fluorescent microspheres and Chinese hamster cells were tested in this system at a throughput between 100 and 200 particles/s.

Recently, Shi et al. (2008) proposed a novel on-chip particle focusing technique using standing surface acoustic waves (SSAW). They deposited a pair of interdigital transducers (IDTs) onto a piezoelectric substrate, between which a polydimethylsiloxane (PDMS)-based microfluidic channel was bonded to the substrate (Fig. 4, left plot). This is different from the previous acoustic focusing designs that used a substrate-bonded bulk transducer within the microchannel to form a resonance cavity. In Shi et al.'s (2008) experiment, 1.9-μm-diameter polystyrene beads were observed to focus into a narrow stream in the center of a 50 × 50 μm channel within 4.5 ms; see Fig. 4 (right plot) for the recorded particle streak images at different sites of the channel. The reported fluid flow velocity is 6.7 cm/s, yielding a flow rate of around 10 μl/min in the microchannel. This SSAW-based focusing method was recently demonstrated by the same group to implement both a diverse patterning (Shi et al. 2009a) and a continuous separation (Shi et al. 2009b) of polymer beads and cells.

While they are simple and efficient, acoustic particle focusers typically require the transducer be in close proximity to the microchannel. This complicates the device fabrication and as well affects its integration with other functional components into lab-on-a-chip devices.

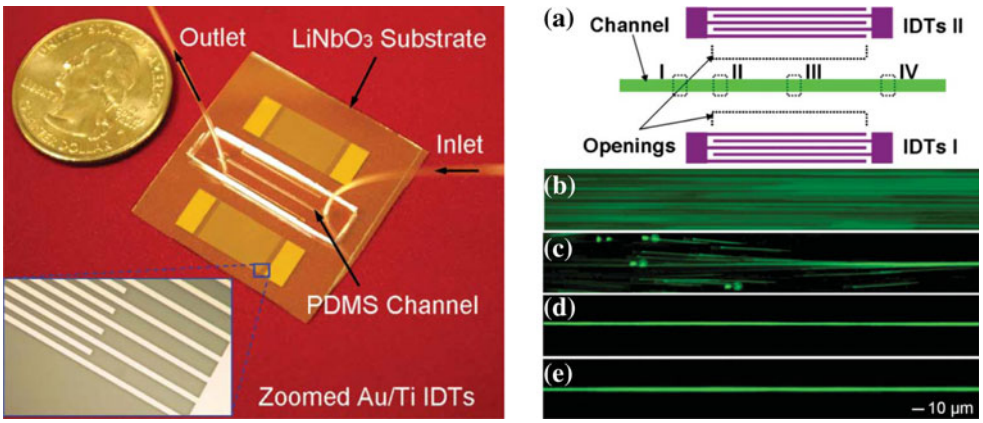

Fig. 4 (*Left*) Photograph of the bonded SSAW focusing device consisting of a $LiNbO_3$ substrate with two parallel IDTs and a PDMS channel; (*right*) recorded fluorescent images of 1.9 μm polystyrene beads at sites (I–IV) of the microchannel. Reprinted from Shi et al. (2008) with permission from Royal Society of Chemistry

Moreover, the acoustic focusing approach is not very suitable for disposable microfluidic devices due to its relatively high cost.

3.1.2 *Axisymmetric flow focusing*

Axisymmetric flow focusing of particles was first demonstrated by Kim and Yoo (2009a) in a 7-cm long circular microcapillary of 85-μm diameter, see Fig. 5 for a schematic. It is based on previous observations that particles lagging behind the Poiseuille flow [e.g., more dense particles in an upflow] migrate toward the tube axis due to an induced "lift" force as illustrated in Fig. 5a (Repetti and Leonard 1964; Jeffrey and Pearson 1965). In Kim and Yoo's experiment, the relative motion between 5-μm-diameter polystyrene beads and the suspending fluid (a solution of water–glycerol mixture with the same density as the particle) was cleverly realized by imposing an electric field in the same direction as the pressure-gradient (Fig. 5b). As negatively charged particles moved electrophoretically against the combined pressure- and electric field-driven fluid flow, they were observed to be focused to the capillary axis at a flow Reynolds number as small as 0.05. Such axisymmetric flow focusing approach was later applied by the same authors (Kim and Yoo 2009b) to focus red blood cells at similar conditions to the focusing of polymer beads; see the two inset images for the unfocused and focused cells. In both experiments, the reported fluid velocity along the capillary centerline (i.e., the maximum flow velocity) is 1.77 mm/s, and the electrophoretic particle velocity is on the order 200 μm/s at a 100 V/cm electric field.

Axisymmetric flow focusing of particles is simple in both principle and control, which, however, requires a relatively long capillary and is thus not suitable for applications based on lab-on-a-chip devices. More importantly, it still needs demonstrations in microfluidic chips fabricated via the standard planar lithography process.

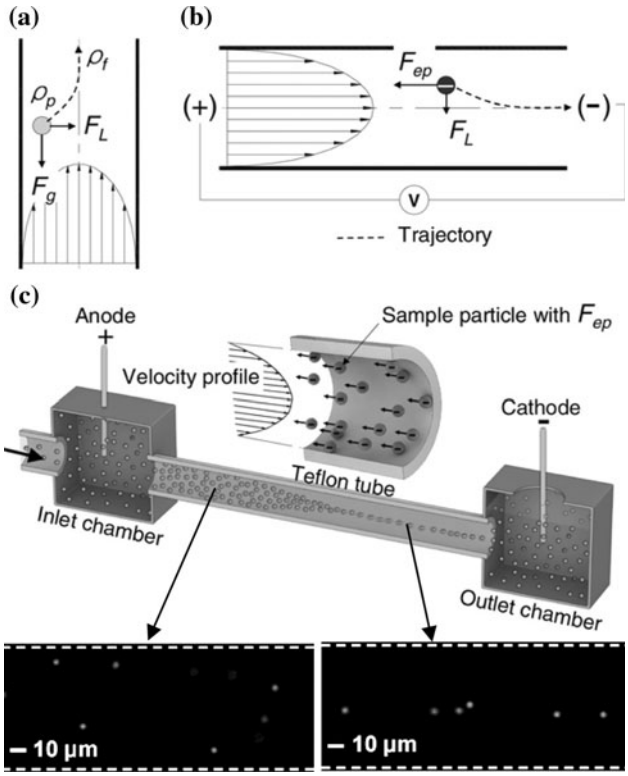

Fig. 5 Schematic of the axisymmetric focusing of particles in a single circular microcapillary. **a** Principle of radially inward migration of non-neutrally buoyant particles; **b** an analogous fluidic situation to **a** where the lagging of particles behind fluid flow is realized by imposing a negative electrophoretic particle motion; **c** schematic of the fluid feeding parts. The two insets at the bottom show the images of unfocused and focused red blood cells. Reprinted from Kim and Yoo (2009a, b) with permissions from Royal Society of Chemistry and Elsevier

3.1.3 *Electrode-based AC dielectrophoretic focusing*

Dielectrophoresis (DEP) is the translational motion of particles due to either the induced (e.g., in polymer beads, cells, viruses, etc.) or native (e.g., in proteins) electrical dipoles in an electric field gradient (Pohl 1978; Morgan and

Green 2002). Therefore, if there exist electric field non-uniformities normal to streamlines, particles can be deflected across the streamlines by DEP and focused to tight stream(s) in the region(s) of balanced forces (Hughes 2002; Gascoyne and Vykoukal 2004).

Traditional dielectrophoretic particle focusing methods are based on the non-uniform AC electric field between pairs of patterned microelectrodes inside microchannels (Lin et al. 2004; Yu et al. 2005; Holmes et al. 2006; Cheng et al. 2007; Lapizco-Encinas and Rito-Palmomares 2007; Demierre et al. 2008; Braschler et al. 2008; Wang et al. 2009). The particle suspension is pumped by a pressure-driven flow. The AC electric voltages must be externally applied to the microelectrodes and must be in the high frequency range in order to reduce the electrode fouling due to electrochemical reactions (Voldman 2006). Such electrode-based AC dielectrophoretic focusing approaches are thus classified into the sub-category of active sheathless particle focusing. In addition, in-channel micro-insulators (e.g., hurdles, posts, ridges, corners, and turns) have also been demonstrated to implement a dielectrophoretic focusing of particle (Chou and Zenhausern 2003; Cummings and Singh 2003; Ozuna-Chacon et al. 2008). In this focusing, the dielectrophoretic force is internally induced around the micro-insulators when a DC field is applied across the entire channel length to transport the particle suspension by electrokinetic flow. Therefore, this insulator-based dielectrophoretic focusing approach is classified into the sub-category of passive sheathless particle focusing and will be presented in Sect. 3.2.4.

To date the majority of the electrode-based dielectrophoretic focusing approaches have used negative DEP (Ateya et al. 2008; Godin et al. 2008). As the largest electric field occurs at the surface of the electrode, particles are pushed away from the electrode. In a recent work, Chu et al. (2009) reported a 3D particle focusing microchannel using positive DEP. As shown schematically in Fig. 6a, a dielectric structure placed between two symmetric planar electrodes induces the maximum electric field at its top edges. Consequently, particles experiencing positive DEP (through tuning the AC voltage frequency) are first forced to travel along the top edges of the dielectric structure, and then focused to the centerline of the microchannel in the pressure-driven laminar wake of the structure. Figure 6b illustrates the images of 2-μm-diameter polystyrene beads near the end of the dielectric structure when the AC voltage (thus positive DEP) is off and on, respectively. The focusing of 4.5 μm polystyrene beads and yeast cells was also tested in this device at a flow rate of 0.01 μl/min, which both showed a weaker focusing efficiency than the 2 μm beads. The geometry of the dielectric structure was later optimized through numerical modeling by Choi et al. (2009a).

For electrode-based AC dielectrophoretic particle focusing, patterning of microelectrodes onto glass or polymeric substrates through metal evaporation or deposition still remains to be challenging and makes the whole device prone to fouling. Moreover, particles must be re-suspended in buffer solutions with a very low ionic concentration in order to suppress Joule heating effects and electrochemical reactions (e.g., generating bubbles and other deleterious chemicals), which may cause adverse effects to bioparticles especially severe to mammalian cells (Voldman 2006). In addition, the focusing efficiency is very sensitive to the particle location as the dielectrophoretic force decays rapidly away from the electrode surfaces (Hughes 2002; Gascoyne and Vykoukal 2004).

3.2 Passive sheathless focusing

3.2.1 Hydrodynamic filtration-based focusing

The concept of "hydrodynamic filtration" was first proposed by Yamada and Seki (2005, 2006) for separating particles by size (Yamada et al. 2007). It is because at a microchannel bifurcation, particles larger than a specific size are excluded from the flow lane near the main channel wall while those smaller than the size are able to follow the

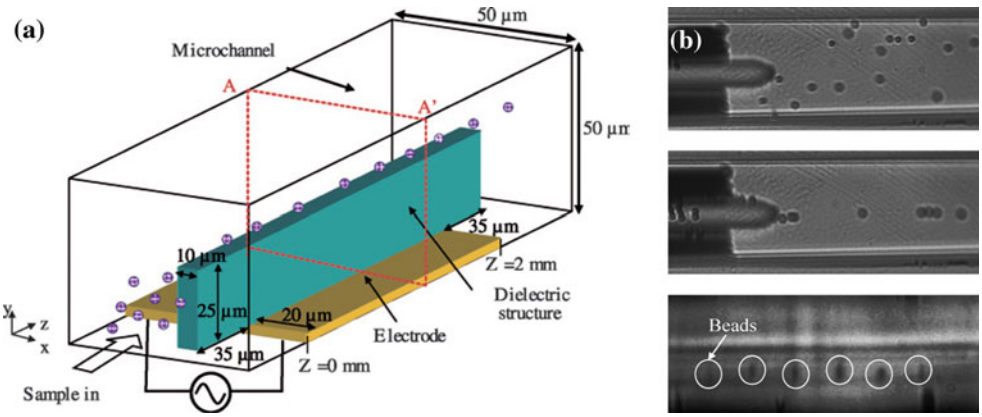

Fig. 6 **a** Schematic view of the 3D particle focusing channel using positive DEP guided by a dielectric structure between two planar electrodes; **b** images of 2 μm polystyrene beads near the end of the focusing channel when the AC voltage is off (*top*) and one (*middle for top view*, *bottom for the side view*). Reprinted from Chu et al. (2009) with permission from Royal Society of Chemistry

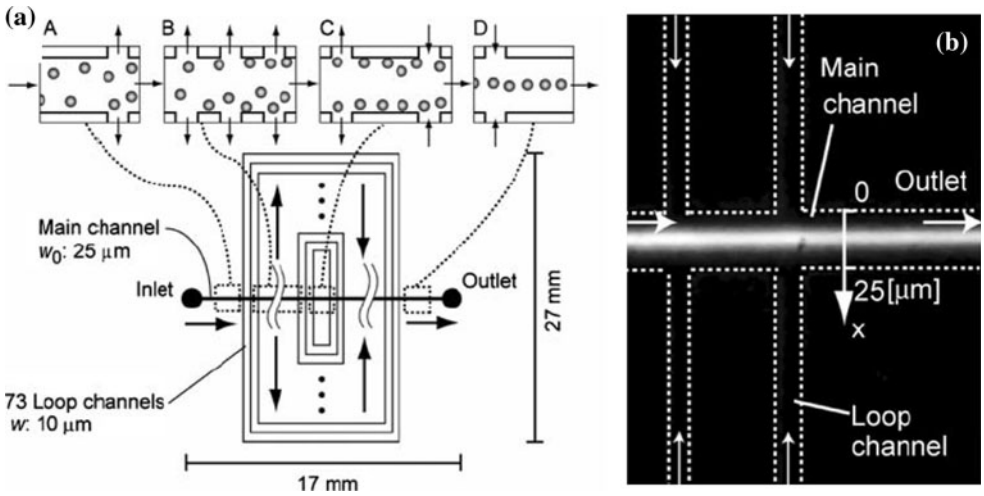

Fig. 7 **a** Principle and microchannel design for hydrodynamic filtration-based focusing of particles. **b** Image of 5 μm fluorescent beads flowing near the outlet of the main channel as indicated in **a**. Reprinted from Aoki et al. (2009) with permission from Springer

flow lane entering into the side channel. This size threshold is determined by the relative flow rate in the main and side channels, which is dependent on the flow resistance and may also be adjusted by tuning the pressure drop in each channel. Hydrodynamic filtration has also been applied to the chemical treatment of cells via a two-step rapid carrier-medium exchange (Yamada et al. 2008).

Recently, Aoki et al. (2009) applied the principle of hydrodynamic filtration to focus particles into a stream along the centerline of a main microchannel. In one of their two designs, as shown in Fig. 7a, multiple loop channels were arranged on both sides of the main channel. These side channels first split the fluid flows from the main channel while leaving particles still in the main stream. Then, these split flows were re-injected into the main stream from both sides simultaneously, serving as sheath flows to focus particles to the center of the main channel instead of its sidewalls. Figure 7b shows an image of 5 μm fluorescent beads flowing near the outlet of the main channel at a flow rate of 2 μl/min.

The positioning and focusing of particles to the channel center were found to be insensitive to the flow speed in Aoki et al.'s experiment (2009). This indicates a potentially high speed operation of the hydrodynamic filtration-based particle focusing device. However, as multiple side channels are necessary for such focusing to work effectively, the device is not appropriate for miniaturization and integration with other components in microfluidic devices.

3.2.2 *Hydrophoretic focusing*

Hydrophoresis indicates the movement of suspended particles in response to a microstructure-induced pressure field. Park's group (Choi and Park 2007; Choi et al. 2007) first harnessed this motion to separate microspheres and cells in a microchannel with fabricated obstacles. The separation takes place due to the size-dependent deflection along the lateral flows induced by the transverse pressure gradients. Such hydrophoretic separation technique has also been applied by the same group to separate submicron beads and DNA molecules by size (Choi et al. 2009b) and as well separate mammalian cells by phase (Choi et al. 2009c).

Recently, Choi et al. (2008) employed hydrophoresis to focus polymer beads and red blood cells to the center of a microchannel. The alternately arranged V-shaped obstacles on the top and bottom channel walls induced lateral pressure gradients, giving rise to two helical recirculations of opposite directions as sketched in Fig. 8a. Therefore, transverse focusing flows were formed as indicated, the result of which was to shift particles to the channel center. Figure 8b shows images of the trajectories of 15 μm beads entering from different cross-sectional positions of the channel with 19.1 μm high V-shaped obstacle arrays. The hydrophoretic drifting of all three beads to the channel center was observed at a flow rate of 0.3 μl/min. A similar principle was demonstrated by Morton et al. (2008) to steer, refract, and focus streams of polystyrene microspheres and blood cells in a microchannel with microfabricated post arrays. The reported flow speed in their device was varied from 50 to 500 μm/s.

More recently, Choi and Park (2008) revised the previous design by using exponentially increasing obstacle arrays. The first section of their new channel utilizes slant obstacles to focus particles to either one sidewall or the channel center based on the symmetry of these obstacles. In the subsequent sections with exponentially increasing channel widths, bent obstacles extended from the slant obstacles maintained the focusing flows and thus increased the particle focusing efficiency. This revised device was demonstrated to implement the hydrophoretic focusing of polystyrene beads of various sizes (6, 10, and 15 μm in diameter) as well as Jurkat

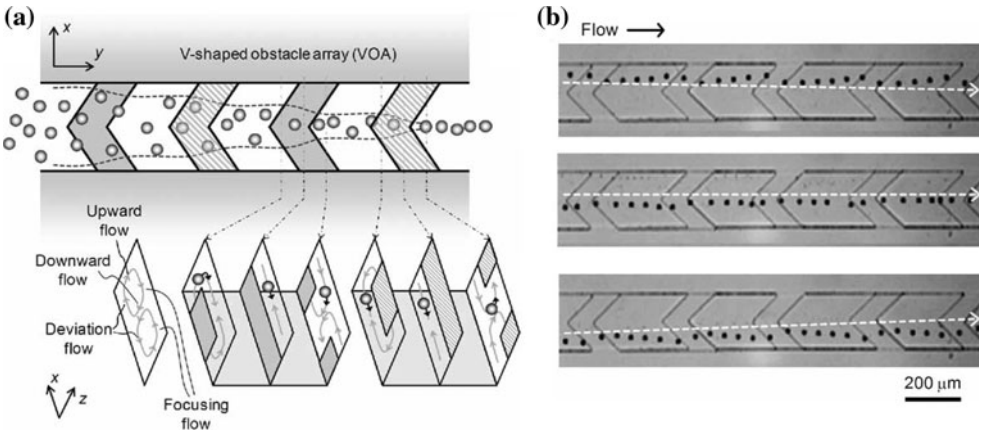

Fig. 8 **a** Schematic diagrams of the microchannel with V-shaped obstacle arrays for hydrophoretic focusing of particles. *Shaded* and *lined areas* denote the lower and upper obstacles, respectively. **b** Images (captured in the first five obstacles) of 15-μm-diameter beads entering from near the left sidewall (*top*), midplane (*middle*), and right sidewall (*bottom*) of the microchannel. Reprinted from Choi et al. (2008) with permission from Wiley

cells at a flow rate of up to 4 μl/min. A similar design was later employed by Hsu et al. (2008) to focus, guide and sort beads and cells. In their design five columns of herringbone grooves were fabricated on the microchannel ceiling to generate microvortices. Particles were trapped and focused to the locations where the flows from adjacent counter-rotating microvortices converge. Moreover, particles heavier or lighter than the suspending fluid were focused to different locations and thus sorted. This device was demonstrated to focus and separate 10 μm poly(methyl methacrylate) and polystyrene beads as well as H1650 cells at a flow velocity of around 3 μm/s (yielding a Reynolds number of ~ 0.01).

Overall, hydrophoretic particle focusing is simple to control. However, the patterning of micro-obstacles on channel walls requires a non-trivial fabrication. Moreover, as the obstacle height needs to be comparable to the particle size for efficient focusing, particle throughput may be limited due to the potentially large probability of clogging.

3.2.3 *Inertial focusing*

Inertial focusing utilizes the cross-stream particle motion to focus particles into one or multiple streams through a microchannel (Di Carlo 2009). The first related experiment was done by Segre and Silberberg (1961), where particles were observed to migrate toward a narrow annulus in a centimeter-scale circular pipe. This so-called "tubular pinch effect" is a result of competition of inertial lift forces acting on particles (Saffman 1965), of which the two dominant ones are the wall lift and the shear-gradient-induced lift (Asmolov 1999; Zeng et al. 2005). Inertial lift forces dominate the particle behavior only when the particle Reynolds number, $Re_p = Re_c d^2/D_h^2$ with Re_c being the traditionally defined channel Reynolds number, d is the particle diameter, and D_h is the channel hydraulic diameter, is of order 1 (Leal 1980). This condition is achievable for particle motion in laminar microfluidic devices. Recently, inertia-induced particle focusing has been experimentally reported in both straight and curved microchannels. These works are reviewed below. More detailed information on developing prototype inertial microfluidic systems for a variety of applications is referred to a very recent review from Di Carlo (2009).

3.2.3.1 Inertial focusing in straight microchannels Di Carlo et al. (2007) were among the first to investigate the inertial focusing of particles in a straight microchannel. They observed that initially uniformly distributed 9-μm-diameter beads were focused to four single streams in a 50-μm-wide square channel when the particle Reynolds number, Re_p, increased to 2.9 (corresponding to the channel Reynolds number, $Re_c = 90$), see Fig. 9b. The four equilibrium positions were all at the centers of the channel faces (see Fig. 9e, f), and were found to move closer to the channel walls as Re_p increased. Recently, Bhagat et al. (2008a) found that the inertial focusing positions of particles in straight microchannels also depend on the channel aspect ratio. They observed that at $Re_p = 0.19$ (corresponding to $Re_c = 20$), 1.9-μm-diameter fluorescent beads were focused to a narrow band along the perimeter, ~ 0.2 D_h away from the walls of a 20×20 μm^2 square channel, which agrees with the finding of Kim and Yoo (2008). At the same Re_c, however, the same particles were aligned along the longer sidewalls of a 20×50 μm^2 rectangular channel, consistent with Di Carlo et al.'s (2009) finding. The latter focusing phenomenon has been recently demonstrated by Bhagat et al. (2009) to continuously filtrate and extract particles from a solution. It has also been demonstrated to implement a controlled encapsulation of single cells into monodisperse drops (Edd et al. 2008) and a sheathless inertial cell ordering for extreme throughput flow cytometry (Hur et al. 2009).

In another study, Park et al. (2009) investigated the inertial focusing of particles in a straight microchannel with 80 alternating narrow (contracting) and wide

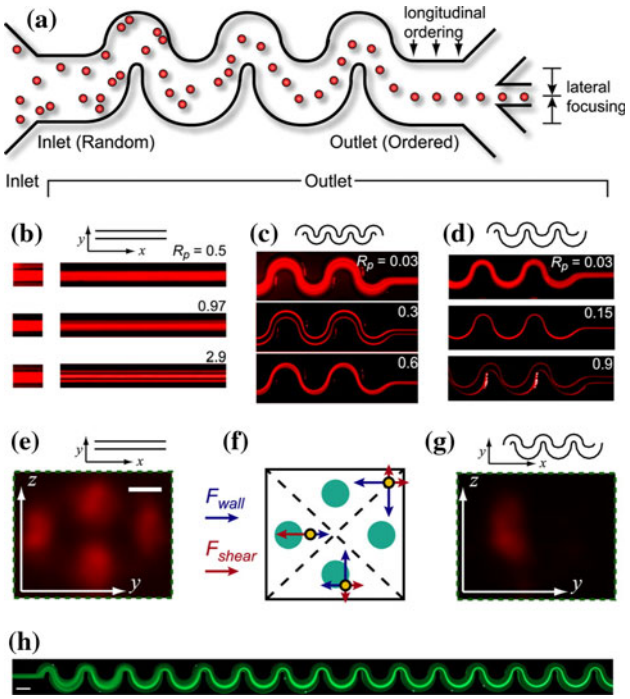

Fig. 9 **a** Schematic drawing of the continuous inertial focusing of particle in a curved microchannel. **b** Top-down views of fluorescent streak images of flowing 9 μm polystyrene beads in a straight square channel. Focusing of particles into four single streamlines is observed. **c** For a symmetric curving channel the symmetry of the system reduces focusing to two streams. **d** For an asymmetric curving system, focusing down to a single stream is favored. **e** A confocal cross-section of the rectangular channel shown in **b** shows focusing of particles to the four channel faces (scale bar, 10 μm). **f** Schematic diagram showing the force balance between the shear-gradient and wall-induced lift for particles in three positions. **g** Confocal cross-section for an asymmetric channel. **h** Starting at the inlet on the left, a random inlet distribution of fluorescent microparticles is focused to a tight streamline on the right after a short distance (scale bar, 160 μm). Reprinted from Di Carlo et al. (2007) with permission from PNAS, National Academy of Sciences

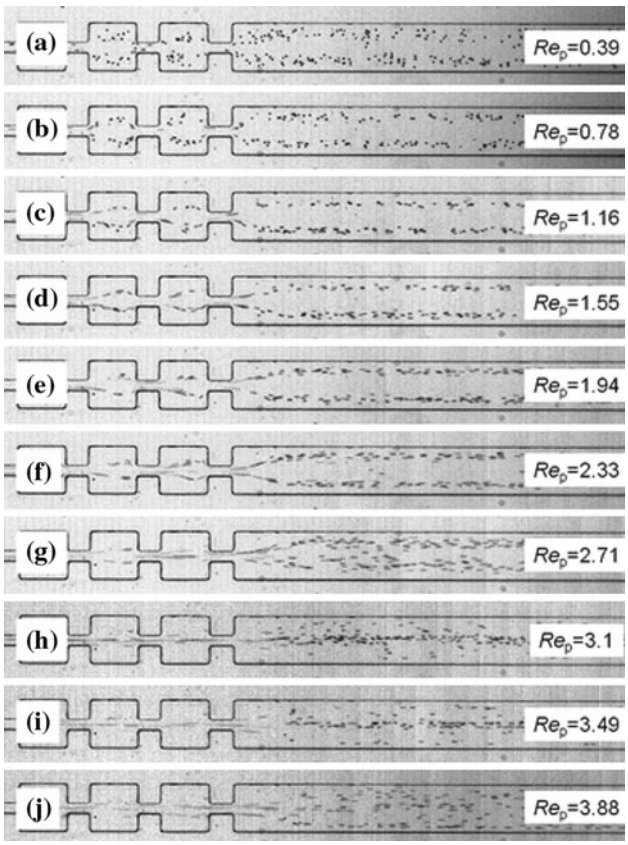

Fig. 10 Inertial focusing of 7 μm polymer beads in a straight multi-orifice microchannel at different particle Reynolds numbers, Re_p. Reprinted from Park et al. (2009) with permission from Royal Society of Chemistry

(expanding) sections in series. The occurrence of vortex flows at the corners of the wide sections modulates the particle focusing positions. Park et al. (2009) observed that 7-μm-diameter polymer microspheres were focused to two lateral positions, $\sim 0.2\, D_h$ away from the channel sidewalls of the last expansion section, as Re_p varied from 0.8 to 2.3 (corresponding to $33 < Re_c < 93$, see Fig. 10b–f). When $3.0 < Re_p < 3.5$, however, particles were focused to a single stream along the channel centerline, as demonstrated in Fig. 10h, i. Similar focusing has been employed by Faivre et al. (2006) to separate blood plasma from blood cells in a straight microchannel with a single geometric constriction.

3.2.3.2 Inertial focusing in curved microchannels Particle inertial focusing in curved microchannels was first studied by Di Carlo et al. (2007), see Fig. 9. When channels are not straight and Reynolds number is not small, a secondary transverse flow or Dean vortex is formed as mentioned earlier (Berger et al. 1983). This double recirculation, as measured by the Dean number, exerts a position-dependent Dean drag force on particles, which biases the particle equilibrium positions. By engineering the microchannel symmetry, Di Carlo et al. (2007) observed that the focusing of 9-μm-diameter beads were reduced from four points in a straight square channel (see Fig. 9b), to two points in a symmetric sinusoidal channel (see Fig. 9c), and then to a single point in an asymmetric sinusoidal channel (see Fig. 9d, g). In the last circumstance, particles were not only focused laterally but also ordered longitudinally in a chain along the flow direction regardless of particle density. Moreover, a fourth dimension of rotational alignment was observed for discoidal red blood cells. These focusing phenomena are, however, all very sensitive to the particle Reynolds number. The reported particle Reynolds number for a single-stream focusing in the asymmetric sinusoidal microchannel was $Re_p \sim 0.2$, yielding a flow rate of ~ 20 μl/min. This inertial focusing has been recently demonstrated by Di Carlo et al. (2008) to separate rigid

particles, deformable emulsions, and platelets from whole blood.

Seo et al. (2007a) studied the inertial focusing of 10.5 μm polystyrene beads in a double-spiral microchannel at the flow velocity varied from 23 to 92 mm/s. The beads were observed to flow in a focused stream nearer to the inner sidewall due to the combined effects of the wall- and shear-gradient-induced lift forces and the curvature-induced centrifugal force and Dean vortices. Both the equilibrium position and the width of the focused particle stream are once again sensitive to the particle Reynolds number. This focusing was later demonstrated by Seo et al. (2007b) to implement a membrane-free separation of particles by size. It has also been used in a sheathless high-throughput flow cytometer (Bhagat et al. 2010). In addition, using the same focusing principle, Bhagat et al. (2008b), Kuntaegowdanahalli et al. (2009), and Russom et al. (2009) have each demonstrated a continuous inertial separation of particles and cells by size in a multi-loop single-spiral microchannel.

Inertia-based particle focusing method is simple and able to offer a very high particle throughput, which, on one hand, makes this method suitable for high-speed applications such as flow cytometry, while on the other hand, poses difficulty on the treatment of rare or precious particles as the particle suspension must flow very fast to induce a decent inertial motion in microchannels. Moreover, as both the number and the equilibrium positions of the focused particle stream(s) are sensitive to the particle Reynolds number, the operation of such inertial particle focusers becomes difficult and complicated. Readers are referred to Gossett and Di Carlo (2009) for a detailed study of the particle focusing mechanism in curving confined microflows.

3.2.4 *Insulator-based dielectrophoretic focusing*

Insulator-based DEP was first demonstrated by Cummings and Singh (2000) in trapping particles through the use of a fabricated array of circular posts. As these posts are electrically insulating, electric field gradients are formed around them, leading to particle DEP (Ai et al. 2009, 2010b). If the induced dielectrophoretic motion can overcome the electrokinetic and Brownian motions, particles are stagnated and concentrated between the posts. This mechanism was later applied to the trapping of biomolecules (Chou et al. 2002; Prinz et al. 2002; Ying et al. 2004; Clarke et al. 2005; Lapizco-Encinas et al. 2008; Gallo-Villanueva et al. 2009), selective concentration/separation of microbial cells (Lapizco-Encinas et al. 2004a, b, 2005; Pysher and Hayes 2007; Cho et al. 2009; Jen and Chen 2008), and continuous separation of polymer beads and biological cells by size (Kang et al. 2006, 2008, 2009; Hawkins et al. 2007; Lewpiriyawong et al. 2008). Insulator-based DEP has also been applied to the continuous focusing of particles (Barrett et al. 2005; Hawkins et al. 2007). Overall two different "insulators" have been demonstrated to generate the required electric field gradients for dielectrophoretic particle focusing: one is the insulating obstacles (e.g., hurdles, posts, and ridges) fabricated inside a microchannel, and the other is the insulating walls of a curved microchannel. These two methods are reviewed separately below.

3.2.4.1 Dielectrophoretic focusing in straight microchannels with micro-obstacles Micro-obstacle-induced dielectrophoretic focusing was first observed in Cummings and Singh's experiment (2003) on streaming DEP of 200-nm latex nanospheres through a microchannel with an array of insulating posts. As the induced positive DEP could not overcome electrokinetic flow, these spheres were drawn to the vertices of the diamond-shaped posts, resulting in highly concentrated particle streams along the columns of the posts. Similar focusing phenomenon was later observed in Xuan et al.'s experiment (2006) where 40 μm beads were focused by negative DEP to the channel centerline after passing through a short 50-μm-wide constriction. As DC electric fields were used in both experiments, the electric field should be large or the particle size should be comparable to the constriction in order to draw sufficient dielectrophoretic motions, where the former condition may cause adverse effects to bioparticles and the latter can significantly increase the probability of device fouling due to particle clogging (Voldman 2006).

Recently, Zhu and Xuan (2009a) demonstrated the use of DC-biased AC electric fields for dielectrophoretic particle focusing in a microchannel constriction. The total field magnitude (i.e., DC plus RMS AC) was maintained at 10 kV/m while the AC to DC electric field ratio was varied from 0 to 9, i.e., from pure DC to 1DC/9AC as indicated in Fig. 11. It was found that 10 μm polystyrene beads were nicely focused to a single line in the channel center at 1DC/9AC, as compared to the slight focusing at pure DC. The enhanced dielectrophoretic focusing in the AC/DC cases is attributed to the increased ratio of the cross-stream particle dielectrophoretic motion to the streamwise electrokinetic motion (Hawkins et al. 2007; Lewpiriyawong et al. 2008). A similar focusing to that at 1DC/9AC was also observed when a 100 kV/m pure DC field was applied, at which the particle speed measured as 6 mm/s in the 310-μm-wide main channel. In addition, oil menisci have been harnessed to shape the electric field for dielectrophoretic particle focusing (Thwar et al. 2007). Superior to the above rigid microstructures, the liquid property of oil provides a flexible and dynamic control of the dimension of the menisci during the experiment. This oil obstacle-induced DEP has

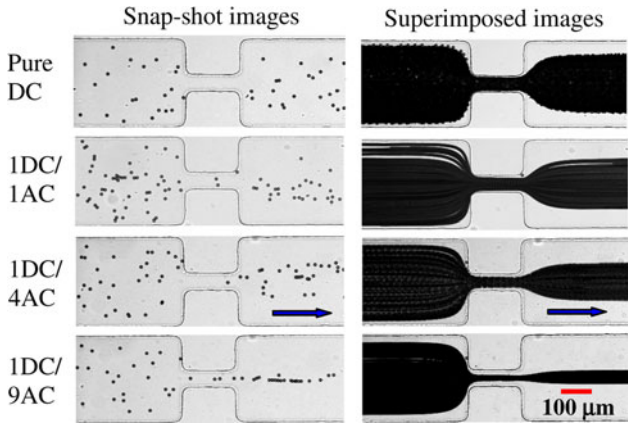

Fig. 11 Micro-obstacle-induced dielectrophoretic focusing of 10 μm polystyrene beads in a 50-μm-wide microchannel constriction at various AC to DC electric field ratios (e.g., 1DC/9AC indicates the ratio of RMS AC to DC field is 9). The total magnitude of the AC (1 kHz frequency) and DC electric fields was maintained at 10 kV/m. The *block arrows* indicate the flow directions. Reprinted from Zhu and Xuan (2009a) with permission from Wiley

also been demonstrated to trap and separate particles (Barbulovic-Nad et al. 2006; Thwar et al. 2007).

Although using DC-biased AC electric fields reduces the field magnitude for obstacle-induced dielectrophoretic particle focusing, the locally amplified electric field around the micro-obstacles may still generate large trans-membrane voltages and shear stresses on cells. Moreover, solutions require being diluted to minimize Joule heating effects. All these conditions may affect the cell viability, especially mammalian cells (Voldman 2006; Lin et al. 2006). In addition, the probability of device failure due to particle clogging or adhesion is also high in microchannels with embedded obstacles.

3.2.4.2 Dielectrophoretic focusing in curved microchannels Xuan's group recently proposed a novel particle focusing technique in DC electrokinetic flow through curved microchannels (Zhu et al. 2009a, b; Church et al. 2009; Zhu and Xuan 2009b). This focusing stems from the cross-stream dielectrophoretic motion induced within the channel turns. Inertia-based lift forces and Dean drag force are both negligible in this dielectrophoretic focusing because the channel Reynolds number, Re_c, is very small under the experimental conditions. Figure 12a shows the electric field lines (equivalent to streamlines with short arrows indicating the directions) and the contour of electric field intensity (the darker the higher) in a round channel turn. Due to the variation in path length, electric field attains the maximum and minimum values near the inner and outer corners of the turn (Ai et al. 2010a; Davison and Sharp 2008), respectively. Therefore, particles will experience a transverse dielectrophoretic motion, $\mathbf{U}_{DEP}$, when they travel electrokinetically, $\mathbf{U}_{EK}$, through the turn. Depending on the relative conductivity between the particle and the suspending fluid, particles may undertake negative (particles are less conductive) or positive (particles are more conductive) DEP and thus be directed toward the outer or inner corner of the turn, as indicated in Fig. 10a.

Zhu et al. (2009a) studied the negative dielectrophoretic focusing of 5 μm polystyrene beads in a 50-μm-wide serpentine microchannel, see Fig. 12b. Due to the alternate switching of inner and outer corners between adjacent U-turns, particles experience periodically switched $\mathbf{U}_{DEP}$ in a serpentine channel. As $\mathbf{U}_{DEP}$ for negative DEP points to the outer corner in each of the turns, particles tend to drift toward the channel center. The overall consequence will thus be a focused particle stream along the channel centerline. This analysis is verified by the observed particle streak images at the entrance and exit regions of the 1-cm long serpentine section (see the insets of Fig. 12b). The average DC electric field across the whole channel was 20 kV/m, which produced an average particle speed of 1.1 mm/s. The larger the electric field, the better focusing can be achieved. The same channel has been recently demonstrated by the same group to implement electrokinetic focusing and filtration of microbial cells (Church et al. 2009).

Zhu et al. (2009b) later examined the dielectrophoretic focusing of 5 μm polystyrene beads in a single-spiral microchannel, see Fig. 12c. The channel is 50-μm wide and

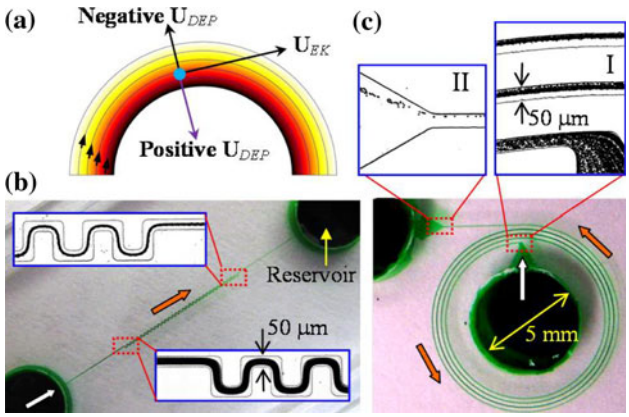

Fig. 12 **a** Illustration of particle electrokinetic and dielectrophoretic motions in a round microchannel turn. **b** Dielectrophoretic focusing of particles in a serpentine microchannel. The two insets show the streak images of 5 μm beads at the entrance and exit of the serpentine section, respectively. Reprinted from Zhu et al. (2009a) with permission from Springer. **c** Dielectrophoretic focusing of particles in a single-spiral microchannel. The insets I and II show the streak image and the snap-shot image of 5 μm beads at the inlet and outlet of the channel, respectively. Reprinted from Zhu et al. (2009b) with permission from ASME. The *block arrows* indicate the flow directions in both **b** and **c**

overall 10-cm long. Different from a serpentine channel, particle DEP in a spiral channel is maintained at a constant angle to the electrokinetic flow as the turn does not change direction over the entire channel. Therefore, particles will be pushed toward the outer wall in every loop via negative DEP, and eventually focused to a stream flowing near the outer channel wall. This is confirmed by the observations of the beads at the inlet and outlet of the spiral channel, see the insets I (superimposed streak images) and II (snap-shot images) in Fig. 10c. Zhu and Xuan (2009b) also studied the dielectrophoretic particle focusing in a double-spiral microchannel. As the induced dielectrophoretic motion depends on the particle size, the dielectrophoretic focusing has been recently demonstrated by Zhu et al. (2010) to implement a continuous separation of particles by size in an asymmetric double-spiral microchannel.

As the curvature-induced dielectrophoretic focusing method excludes the use of micro-obstacles inside microchannels, the device is less prone to fouling (due to particle clogging and/or locally amplified electric fields) than the one based on micro-obstacles. However, both methods still suffer from the restriction of low particle throughput because electrokinetic flow is typically limited to just a few mm/s. Moreover, such insulator-based dielectrophoretic focusing is sensitive to the contaminations on channel walls due to, for example, the adhesion of particles. This is because any surface inhomogeneity can easily cause disturbances to the electroosmotic flow for particle suspension pumping (Anderson 1989).

4 Conclusions and outlook

Various sheath flow and sheathless approaches to particle focusing in microfluidic devices have been reviewed in this article. They are also summarized in Table 1 with details of the particle and flow information from the selected references. Each approach has its own advantages and disadvantages, so the comparison of performance is not always straightforward. The selection of the optimum method will depend on the needs of the application which may cover efficiency, reliability, simplicity, throughput and physiological effects, etc. The integration of particle focusing techniques with pre- and post-focusing processes onto a

Table 1 Listing of microfluidic particle focusing methods with details of the basis of particle focusing, the applicable particles (including type and size), and the data for flow rates in the selected references

Classification	Methods	Focusing induced by	Particle	Flow rate	Refs.
Sheath flow focusing	Using grooved microchannels	Sheath fluid and lateral transport	5.6 μm polystyrene beads	10 μl/min	Golden et al. (2009)
	Dean flow assisted	Sheath fluid and Dean vortices	Red blood cells	0.1 ml/h	Lee et al. (2009)
	With vertical confinement	Horizontal and vertical sheaths	T lymphocytes	4 μl/min	Watkins et al. (2009)
Sheathless focusing					
Active	Acoustic	Acoustic force	1.9 μm polystyrene beads	10 μl/min	Shi et al. (2008)
	Axisymmetric flow	Velocity gradient-induced lift force	5 μm polystyrene beads, red blood cells	0.5 μl/min	Kim and Yoo (2009a, b)
	Electrode-based AC dielectrophoretic	Externally controlled DEP	Polystyrene beads and yeast cells	0.01 μl/min	Chu et al. (2009)
Passive	Hydrodynamic filtration	Laminar flow	5 μm polystyrene beads	2 μl/min	Aoki et al. (2009)
	Hydrophoretic	Lateral circulations	Polystyrene beads and Jurkat cells	4 μl/min	Choi and Park (2008)
	Inertial				
	Straight microchannels	Inertial lift forces	7 μm polystyrene beads	140 μl/min	Park et al. (2009)
	Curved microchannels	Inertial lift and Dean drag forces	Beads, oil droplets, and red blood cells	~20 μl/min	Di Carlo et al. (2007)
	Insulator-based dielectrophoretic				
	Straight microchannels	Internally induced DEP by channel topology	Polystyrene beads	5 μl/min	Zhu and Xuan (2009a)
	Curved microchannels		Polystyrene beads	0.1 μl/min	Zhu and Xuan (2009b)

single chip will be the ultimate goal of future research and development. The resultant lab-on-a-chips or micro-total-analysis-systems will find applications in many areas such as agriculture, biomedicine, environment, food technology, and the pharmaceutical industry.

Acknowledgements This work was supported by NSF under grant CBET-0853873 with Marc S. Ingber as the grant monitor. The support from Clemson University through a startup package to Xuan, the Creative Inquiry Program, and the Research Investment Initiative Fund Program is also gratefully acknowledged.

References

Ai Y, Joo SW, Jiang Y, Xuan X, Qian S (2009) Transient electrophoretic motion of a charged particle through a converging-diverging microchannel: effect of direct current dielectrophoretic force. Electrophoresis 30:2499–2506

Ai Y, Park S, Zhu J, Xuan X, Beskok A, Qian S (2010a) DC electrokinetic particle transport in an L-shaped microchannel. Langmuir 26:2937–2944

Ai Y, Qian S, Liu S, Joo SW (2010b) Dielectrophoretic choking phenomenon in a converging-diverging microchannel. Biomicrofluidics 4:013201

Anderson JL (1989) Colloid transport by interfacial forces. Annu Rev Fluid Mech 21:61–99

Aoki R, Yamada M, Yasuda M, Seki M (2009) In-channel focusing of flowing microparticles utilizing hydrodynamic filtration. Microfluid Nanofluid 6:571–576

Asmolov ES (1999) The inertial lift on a spherical particle in a plane Poiseuille flow at large channel Reynolds number. J Fluid Mech 381:63–87

Ateya DA, Erickson JS, Howell PB Jr, Hilliard LR, Golden JP, Ligler FS (2008) The good, the bad, and the tiny: a review of microflow cytometry. Anal Bioanal Chem 391:1485–1498

Barbulovic-Nad I, Xuan X, Lee JSH, Li D (2006) DC-dielectrophoretic separation of microparticles using an oil droplet obstacle. Lab Chip 6:274–279

Barrett LM, Skulan AJ, Singh AK, Cummings EB, Fiechtner GJ (2005) Dielectrophoretic manipulation of particles and cells using insulating ridges in faceted prism microchannels. Anal Chem 77:6798–6804

Berger A, Talbot L, Yao LS (1983) Flow in curved pipes. Annu Rev Fluid Mech 15:461–512

Bhagat AAS, Kuntaegowdanahalli SS, Papautsky I (2008a) Enhanced particle filtration in straight microchannels using shear-modulated inertial migration. Phys Fluid 20:101702

Bhagat AAS, Kuntaegowdanahalli SS, Papautsky I (2008b) Continuous particle separation in spiral microchannels using dean flows and differential migration. Lab Chip 8:1906–1914

Bhagat AAS, Kuntaegowdanahalli SS, Papautsky I (2009) Inertial microfluidics for continuous particle filtration and extraction. Microfluid Nanofluid 7:221–230

Bhagat AAS, Kuntaegowdanahalli SS, Papautsky I (2010) Inertial microfluidics for sheath-less high-throughput flow cytometry. Biomed Microdev. doi:10.1007/s10544-009-9374-9

Braschler T, Demierre N, Nascimento E, Silva T, Oliva AG, Renaud P (2008) Continuous separation of cells by balanced dielectrophoretic forces at multiple frequencies. Lab Chip 8:280–286

Chang CC, Huang ZY, Yang RJ (2007) Three-dimensional hydrodynamic focusing in two-layer polydimethylsiloxane (PDMS) microchannels. J Micromech Microeng 17:1479–1486

Chau LK, Osborn T, Wu CC, Yager P (1999) Microfabricated silicon flow-cell for optical monitoring of biological fluids. Anal Sci 15:721–724

Cheng IF, Chang HC, Hou D, Chang HC (2007) An integrated dielectrophoretic chip for continuous bioparticle filtering, focusing, sorting, trapping, and detecting. Biomicrofluidics 1:021503 (1–15)

Cho YK, Kim S, Lee K, Park C, Lee JG, Ko C (2009) Bacteria concentration using a membrane type insulator-based dielectrophoresis in a plastic chip. Electrophoresis 30:3153–3159

Choi S, Park JK (2007) Continuous hydrophoretic separation and sizing of microparticles using slanted obstacles in a microchannel. Lab Chip 7:890–897

Choi S, Park JK (2008) Sheathless hydrophoretic particle focusing in a microchannel with exponentially increasing obstacle arrays. Anal Chem 80:3035–3039

Choi S, Song S, Choi C, Park JK (2007) Continuous blood cell separation by hydrophoretic filtration. Lab Chip 7:1532–1538

Choi S, Song S, Choi C, Park JK (2008) Sheathless focusing of microbeads and blood cells based on hydrophoresis. Small 4:634–641

Choi KH, Rehmani MAA, Doh I, Cho Y (2009a) Numerical study of particle focusing through improved lab-on-a-chip device by positive dielectrophoresis. Microsyst Technol 15:1059–1065

Choi S, Song S, Choi C, Park JK (2009b) Hydrophoretic sorting of micrometer and submicrometer particles using anisotropic microfluidic obstacles. Anal Chem 81:50–55

Choi S, Song S, Choi C, Park JK (2009c) Microfluidic self-sorting of mammalian cells to achieve cell cycle synchrony by hydrophoresis. Anal Chem 81:1964–1968

Chou CF, Zenhausern F (2003) Electrodeless dielectrophoresis for micro total analysis systems. IEEE Eng Med Biol Mag 22:62–67

Chou CF, Tegenfeldt JO, Bakajin O, Chan SS, Cox EC, Darnton N, Duke T, Austin RH (2002) Electrodeless dielectrophoresis of single- and double-stranded DNA. Biophys J 83:2170–2179

Chu H, Doh I, Cho Y (2009) A three-dimensional (3D) particle focusing channel using the positive dielectrophoresis (pDEP) guided by a dielectric structure between two planar electrodes. Lab Chip 9:686–691

Chung TD, Kim HC (2007) Recent advances in miniaturized microfluidic flow cytometry for clinical use. Electrophoresis 28:4511–4520

Church C, Zhu J, Wang G, Tzeng TJ, Xuan X (2009) Electrokinetic focusing and filtration of cells in a serpentine microchannel. Biomicrofluidics 3:044109

Clarke RW, White SS, Zhou D, Ying L, Klenerman D (2005) Trapping of proteins under physiological conditions in a nanopipette. Angew Chem 44:3747–3750

Cummings EB, Singh AK (2000) Dielectrophoretic trapping without embedded electrodes. In: Proceedings of SPIE conference micromachining microfabrication, vol 4177, pp 164–173

Cummings EB, Singh AK (2003) Dielectrophoresis in microchips containing arrays of insulating posts: theoretical and experimental results. Anal Chem 75:4724–4731

Davison SM, Sharp KV (2008) Transient simulations of the electrophoretic motion of a cylindrical particle through a 90° corner. Microfluid Nanofluid 4:409–418

Demierre N, Braschler T, Muller R (2008) Focusing and continuous separation of cells in a microfluidic device using lateral dielectrophoresis. Sens Actuators B 132:388–396

Di Carlo D (2009) Inertial microfluidics. Lab Chip 9:3038–3046

Di Carlo D, Irimia D, Tompkins RG, Toner M (2007) Continuous inertial focusing, ordering, and separation of particles in microchannels. Proc Natl Acad Sci 104:18892–18897

Di Carlo D, Edd JF, Irimia D, Tompkins RG, Toner M (2008) Equilibrium separation and filtration of particles using differential inertial focusing. Anal Chem 80:2204–2211

Di Carlo D, Edd JF, Humphry KJ, Stone HA, Toner M (2009) Particle segregation and dynamics in confined flows. Phys Rev Lett 102:094503

Edd JF, Di Carlo D, Humphry KJ, Koester S, Irimia D, Weitz DA, Toner M (2008) Controlled encapsulation of single-cells into monodisperse picolitre drops. Lab Chip 8:1262–1264

Faivre M, Abkarian M, Bickraj K, Stone HA (2006) Geometrical focusing of cells in a microfluidic device: an approach to separate blood plasma. Biorheology 43:147–159

Fu AY, Spence C, Scherer A, Arnold FH, Quake SRA (1999) Microfabricated fluorescence-activated cell sorter. Nat Biotechnol 17:1109–1111

Fu LM, Yang RJ, Lin C, Pan Y, Lee GB (2004) Electrokinetically driven micro flow cytometers with integrated fiber optics for on-line cell/particle detection. Anal Chim Acta 507:163–169

Fu LM, Tsai CH, Lin CH (2008) A high-discernment microflow cytometer with microweir structure. Electrophoresis 29:1874–1880

Gallo-Villanueva RC, Rodriguez-Lopez CE, Diaz-de-la-Garza RI, Reyes-Betanzo C, Lapizco-Encinas BH (2009) DNA manipulation by means of insulator-based dielectrophoresis employing direct current electric fields. Electrophoresis 30:4195–4205

Gascoyne PRC, Vykoukal JV (2002) Particle separation by dielectrophoresis. Electrophoresis 23:1973–1983

Gascoyne PRC, Vykoukal JV (2004) Dielectrophoresis-based sample handling in general-purpose programmable diagnostic instruments. Proc IEEE 92:22–42

Goddard GR, Martin JC, Graves SW, Kaduchak G (2006) Ultrasonic particle concentration for sheath-less focusing of particles for analysis in a flow cytometer. Cytometry 69A:66–74

Goddard GR, Sanders CK, Martin JC, Kaduchak G, Graves SW (2007) Analytical performance of an ultrasonicparticle focusing flow cytometer. Anal Chem 79:8740–8746

Godin J, Chen C, Cho SH, Qiao W, Tsai F, Lo Y (2008) Microfluidics and photonics for bio-system-on-a-chip: a review of advancements in technology towards a microfluidic flow cytometry chip. J Biophoton 1:355–376

Golden JP, Kim JS, Erickson JS, Hilliard LR, Howell PB, Anderson GP, Nasir M, Ligler FS (2009) Multi-wavelength microflow cytometer using groove-generated sheath flow. Lab Chip 9:1942–1950

Gossett DR, Di Carlo D (2009) Particle focusing mechanisms in curving confined flows. Anal Chem 81:2459–2465

Hairer G, Vellekoop MJ (2009) An integrated flow-cell for full sample stream control. Microfluid Nanofluid 7:647–658

Hairer G, Parr GS, Svasek P, Jachimowicz A, Vellekoop MJ (2008) Investigations of micrometer sample stream profiles in a three-dimensional hydrodynamic focusing device. Sens Actuators B 132:518–524

Hawkins BG, Smith AE, Syed YA, Kirby BJ (2007) Continuous-flow particle separation by 3D insulative dielectrophoresis using coherently shaped, DC-biased, AC electric fields. Anal Chem 79:7291–7300

Holmes D, Morgan H, Green NG (2006) High throughput particle analysis: combining dielectrophoretic particle focusing with confocal optical detection. Biosens Bioelectron 21:1621–1630

Hou HH, Tsai CH, Fu LM, Yang RJ (2009) Experimental and numerical investigation into micro-flow cytometer with 3-D hydrodynamic focusing effect and micro-weir structure. Electrophoresis 30:2507–2515

Howell PB, Golden JP, Hilliard LR, Erickson JS, Mott DR, Ligler FS (2008) Two simple and rugged designs for creating microfluidic sheath flow. Lab Chip 8:1097–1103

Hsu CH, Di Carlo D, Chen CC, Irimia D, Toner M (2008) Microvortex for focusing, guiding and sorting of particles. Lab Chip 8:2128–2134

Hughes MP (2002) Strategies for dielectrophoretic separation in laboratory-on-a-chip systems. Electrophoresis 23:2569–2582

Huh D, Gu W, Kamotani Y, Grotgerg JB, Takayama S (2005) Microfluidics for flow cytometric analysis of cells and particles. Physiol Meas 26:R73–R98

Hur SC, Tse HTK, Di Carlo D (2009) Sheathless inertial cell ordering for extreme throughput flow cytometry. Lab Chip. doi: 10.1039/b919495a

Jeffrey RC, Pearson JRA (1965) Particle motion in laminar vertical tube flow. J Fluid Mech 22:721–735

Jen CP, Chen TW (2008) Selective trapping of live and dead mammalian cells using insulator-based dielectrophoresis within open-top microstructures. Biomed Microdev 11:597–607

Kang K, Kang Y, Xuan X, Li D (2006) Continuous separation of microparticles by size with DC-dielectrophoresis. Electrophoresis 27:694–702

Kang Y, Li D, Kalams SA, Eid JE (2008) DC-dielectrophoretic separation of biological cells by size. Biomed Microdev 10:243–249

Kang Y, Cetin B, Wu Z, Li D (2009) Continuous particle separation with localized AC-dielectrophoresis using embedded electrodes and an insulating hurdle. Electrochim Acta 54:1715–1720

Kersaudy-Kerhoas M, Dhariwal R, Desmulliez MPY (2008) Recent advances in microparticle continuous separation. IET Nanobiotechnol 2:1–13

Kim YW, Yoo JY (2008) The lateral migration of neutrally-buoyant spheres transported through square microchannels. J Micromech Microeng 18:065015(1–13)

Kim YW, Yoo JY (2009a) Axisymmetric flow focusing of particles in a single microchannel. Lab Chip 9:1043–1045

Kim YW, Yoo JY (2009b) Three-dimensional focusing of red blood cells in microchannels for bio-sensing applications. Biosens Bioelectron 24:3677–3682

Kim JS, Anderson GP, Erickson JS, Golden JP, Nasir M, Ligler FS (2009) Multiplexed detection of bacteria and toxins using a microflow cytometer. Anal Chem 81:5426–5432

Kohlheyer D, Unnikrishnan S, Besselink GAJ, Schlautmann S, Schasfoort RBM (2008) A microfluidic device for array patterning by perpendicular electrokinetic focusing. Microfluid Nanofluid 4:557–564

Kulrattanarak T, van der Sman RGM, Schroen CGPH, Boom RM (2008) Classification and evaluation of microfluidic devices for continuous suspension fractionation. Adv Colloid Interface Sci 142:53–65

Kummrow A, Theisen J, Frankowski M, Tuchscheerer A, Yildirim H, Brattke K, Schmidt M, Neukammer J (2009) Microfluidic structures for flow cytometric analysis of hydrodynamically focussed blood cells fabricated by ultraprecision micromachining. Lab Chip 9:972–981

Kuntaegowdanahalli S, Bhagat AAS, Kumar G, Papautsky I (2009) Inertial microfluidics for continuous particle separation in spiral microchannels. Lab Chip 9:2973–2980

Lapizco-Encinas BH, Rito-Palmomares M (2007) Dielectrophoresis for the manipulation of nanoparticles. Electrophoresis 28:4521–4538

Lapizco-Encinas BH, Simmons BA, Cummings EB, Fintschenko Y (2004a) Dielectrophoretic concentration and separation of live and dead bacteria in an array of insulators. Anal Chem 76:1571–1579

Lapizco-Encinas BH, Simmons BA, Cummings EB, Fintschenko Y (2004b) Insulator-based dielectrophoresis for the selective concentration and separation of live bacteria in water. Electrophoresis 25:1695–1704

Lapizco-Encinas BH, Davalos RV, Simmons BA, Cummings EB, Fintschenko Y (2005) An insulator-based (electrodeless) dielectrophoretic concentrator for microbes in water. J Microbiol Method 62:317–326

Lapizco-Encinas BH, Ozuna-Chacon S, Rito-Palomares M (2008) Protein manipulation with insulator-based dielectrophoresis and DC electric fields. J Chromatogr A 1206:45–51
Leal LG (1980) Particle motions in a viscous fluid. Annu Rev Fluid Mech 12:435–476
Lee GB, Lin C, Chang G (2003) Micro flow cytometers with buried SU-8/SOG optical waveguides. Sens Actuators A 103:165–170
Lee GB, Chang CC, Huang SB, Yang RJ (2006) The hydrodynamic focusing effect in rectangular microchannels. J Micromech Microeng 16:1024–1032
Lee MG, Choi S, Park JK (2009) Three-dimensional hydrodynamic focusing with a single sheath flow in a single-layer microfluidic device. Lab Chip 9:3155–3160
Lewpiriyawong N, Yang C, Lam YC (2008) Dielectrophoretic manipulation of particles in a modified microfluidic H-Filter with multi-insulating blocks. Biomicrofluidics 2:034105
Lin CH, Lee GB, Fu LM, Hwey BH (2004) Vertical focusing device utilizing dielectrophoretic force and its application on microflow cytometer. J Microelectromech Syst 13:923–932
Lin R, Ho C, Liu C, Chang H (2006) Dielectrophoresis based-cell patterning for tissue engineering. Biotechnol J 1:949–957
Liu C, Stakenborg T, Peeters S, Lagae L (2009) Cell manipulation with magnetic particles toward microfluidic cytometry. J Appl Phys 105:102014
Mao X, Huang TJ (2008) Focusing fluids and light in micro/nano scale—enabling technologies for single-particle detection. IEEE Nanotechnol Mag 2:22–27
Mao X, Waldeisen JR, Huang TJ (2007) "Microfluidic drifting"—implementing three-dimensional hydrodynamic focusing with a single-layer planar microfluidic device. Lab Chip 7:1260–1262
Mao X, Lin SS, Dong C, Huang TJ (2009) Single-layer planar on-chip flow cytometer using microfluidic drifting based three-dimensional (3D) hydrodynamic focusing. Lab Chip 9:1583–1589
Morgan H, Green NG (2002) AC electrokinetics: colloids and nanoparticles. Research Studies Press, Hertfordshire
Morton KJ, Loutherback K, Inglis DW, Tsui OK, Sturm JC, Chou SY, Austin RH (2008) Hydrodynamic metamaterials: microfabricated arrays to steer, refract, and focus streams of biomaterials. Proc Natl Acad Sci 105:7434–7438
Ozuna-Chacon S, Lapizco-Encinas BH, Rito-Palomares M, Martínez-Chapa SO, Reyes-Betanzo C (2008) Performance characterization of an insulator-based dielectrophoretic microdevice. Electrophoresis 29:3115–3122
Pamme N (2007) Continuous flow separations in microfluidic devices. Lab Chip 7:1644–1659
Park J, Song S, Jung H (2009) Continuous focusing of microparticles using inertial lift force and vorticity via multi-orifice microfluidic channels. Lab Chip 9:939–948
Petersson F, Nilsson A, Jonsson H, Laurell T (2005) Carrier medium exchange through ultrasonic particle switching in microfluidic channels. Anal Chem 77:1216–1221
Petersson F, Aberg L, Sword-Nilsson AM, Laurell T (2007) Free flow acoustophoresis: microfluidic-based mode of particle and cell separation. Anal Chem 79:5117–5123
Pohl HA (1978) Dielectrophoresis. Cambridge University Press, Cambridge
Prinz C, Tegenfeldt JO, Austin RH, Cox EC, Sturm JC (2002) Bacterial chromosome extraction and isolation. Lab Chip 2:207–212
Pysher MD, Hayes MA (2007) Electrophoretic and dielectrophoretic field gradient technique for separating bioparticles. Anal Chem 79:4552–4557
Repetti RV, Leonard EF (1964) Segré-Silberberg annulus formation: a possible explanation. Nature 203:1346–1348
Rodriguez-Trujillo R, Mills CA, Samitier J, Gomila G (2007) Low cost micro-Coulter counter with hydrodynamic focusing. Microfluid Nanofluid 3:171–176
Russom A, Gupta AK, Nagrath S, Di Carlo D, Edd JF, Toner M (2009) Differential inertial focusing of particles in curved low-aspect-ratio microchannels. New J Phys 11:075025
Saffman PG (1965) The lift on a small sphere in a slow shear flow. J Fluid Mech 22:385–400
Scott R, Sethu P, Harnett CK (2008) Three-dimensional hydrodynamic focusing in a microfluidic Coulter counter. Rev Sci Instrum 79:046104
Segre G, Silberberg A (1961) Radial particle displacements in Poiseuille flow of suspensions. Nature 189:209–210
Seo J, Lean MH, Kole A (2007a) Membrane-free microfilltration by asymmetric inertial migration. Appl Phys Lett 91:033901
Seo J, Lean MH, Kole A (2007b) Membraneless microseparation by asymmetry in curvilinear laminar flows. J Chromatogr A 1162:126–131
Shi J, Mao X, Ahmed D, Colletti A, Huang TJ (2008) Focusing microparticles in a microfluidic channel with standing surface acoustic waves (SSAW). Lab Chip 8:221–223
Shi J, Ahmed D, Mao D, Lin SS, Huang TJ (2009a) Acoustic tweezers: patterning cells and microparticles using standing surface acoustic waves (SSAW). Lab Chip 9:2890–2895
Shi J, Huang H, Stratton Z, Lawit A, Huang Y, Huang TJ (2009b) Continuous particle separation in a microfluidic channel via standing surface acoustic waves (SSAW). Lab Chip 9:3354–3359
Sims CE, Allbritton NL (2007) Analysis of single mammalian cells on-chip. Lab Chip 7:423–440
Tanaka Y, Sato K, Shimizu T, Yamato M, Okano T, Kitamori T (2007) Biological cells on microchips: new technologies and applications. Biosens Bioelectron 23:449–458
Thwar PK, Linderman JJ, Burns MA (2007) Electrodeless direct current dielectrophoresis using reconfigurable field-shaping oil barriers. Electrophoresis 28:4572–4581
Toner M, Irimia D (2005) Blood-on-a-chip. Annu Rev Biomed Eng 7:77–103
Tsai CG, Hou HH, Fu LM (2008) An optimal three-dimensional focusing technique for micro-flow cytometers. Microfluid Nanofluid 5:827–836
Tsutsui H, Ho CM (2009) Cell separation by non-inertial force fields in microfluidic systems. Mech Res Commun 36:92–103
Voldman J (2006) Electrical forces for microscale cell manipulation. Annu Rev Biomed Eng 8:425–454
Wang L, Lu J, Marchenko SA, Monuki ES, Flanagan LA, Lee AP (2009) Dual frequency dielectrophoresis with interdigitated sidewall electrodes for microfluidic flow-through separation of beads and cells. Electrophoresis 30:1–10
Watkins N, Venkatesan BM, Toner M, Rodriguez W, Bashir R (2009) A robust electrical microcytometer with 3-dimensional hydrofocusing. Lab Chip 9:3177–3184
Xuan X, Li D (2005) Focused electrophoretic motion and selected electrokinetic dispensing of particles and cells in cross-microchannels. Electrophoresis 26:3552–3560
Xuan X, Raghibizadeh S, Li D (2006) Wall effects on electrophoretic motion of spherical polystyrene particles in a rectangular poly(dimethylsiloxane) microchannel. J Colloid Interface Sci 296:743–748
Yamada M, Seki M (2005) Hydrodynamic filtration for on-chip particle concentration and classification utilizing microfluidics. Lab Chip 5:1233–1239
Yamada M, Seki M (2006) Microfluidic particle sorter employing flow splitting and recombining. Anal Chem 78:1357–1362
Yamada M, Kano K, Tsuda Y, Kobayashi J, Yamato M, Seki M, Okano T (2007) Microfluidic devices for size-dependent separation of liver cells. Biomed Microdev 9:637–645
Yamada M, Kobayashi J, Yamato M, Seki M, Okano T (2008) Millisecond treatment of cells using microfluidic devices via two-step carrier-medium exchange. Lab Chip 8:772–778

Yang RJ, Chang CC, Huang SB, Lee GB (2005) A new focusing model and switching approach for electrokinetic flow inside microchannels. J Micromech Microeng 15:2141–2148

Yi CQ, Li CW, Ji SL, Yang MS (2006) Microfluidics technology for manipulation and analysis of biological cells. Anal Chim Acta 560:1–23

Ying LM, White SS, Bruckbauer A, Meadows L, Korchev YE, Klenerman D (2004) Frequency and voltage dependence of the dielectrophoretic trapping of short lengths of DNA and dCTP in a nanopipette. Biophys J 86:1018–1027

Yu C, Vykoukal J, Vykoukal DM, Schwartz JA, Shi L, Gascoyne PRC (2005) A three-dimensional dielectrophoretic particle focusing channel for microcytometry applications. J Microelectromech Syst 14:480–487

Zeng L, Balachandar S, Fischer P (2005) Wall-induced forces on a rigid sphere at finite Reynolds number. J Fluid Mech 536:1–25

Zhao Y, Fujimoto BS, Jeffries GDM, Schiro PG, Chiu DT (2007) Optical gradient flow focusing. Opt Express 15:6167–6176

Zhu J, Xuan X (2009a) Dielectrophoretic focusing of particles in a microchannel constriction using DC-biased AC electric fields. Electrophoresis 30:2668–2675

Zhu J, Xuan X (2009b) Particle electrophoresis and dielectrophoresis in curved microchannels. J Colloid Interface Sci 340:285–290

Zhu J, Tzeng TR, Hu G, Xuan X (2009a) DC dielectrophoretic focusing of particles in a serpentine microchannel. Microfluid Nanofluid 7:751–756

Zhu J, Tzeng JT, Xuan X (2009b) Dielectrophoretic focusing of microparticles in curved microchannels. In: Proceedings of the ASME 2009 international mechanical engineering congress and exposition, IMECE2009-11876, Lake Buena Vista, FL

Zhu J, Tzeng TR, Xuan X (2010) Continuous dielectrophoretic separation of particles in a spiral microchannel. Electrophoresis. doi:10.1002/elps.200900736 (in press)